The Company of Biologists

RESEARCH ARTICLE

FGF signaling refines Wnt gradients to regulate the patterning of taste papillae

Michaela Prochazkova[1,2], Teemu J. Häkkinen[3], Jan Prochazka[1,2], Frantisek Spoutil[2], Andrew H. Jheon[1], Youngwook Ahn[4], Robb Krumlauf[4,5], Jukka Jernvall[3,*] and Ophir D. Klein[1,6,*]

ABSTRACT

The patterning of repeated structures is a major theme in developmental biology, and the inter-relationship between spacing and size of such structures is an unresolved issue. Fungiform papillae are repeated epithelial structures that house taste buds on the anterior tongue. Here, we report that FGF signaling is a crucial regulator of fungiform papillae development. We found that mesenchymal FGF10 controls the size of the papillary area, while overall patterning remains unchanged. Our results show that FGF signaling negatively affects the extent of canonical Wnt signaling, which is the main activation pathway during fungiform papillae development; however, this effect does not occur at the level of gene transcription. Rather, our experimental data, together with computational modeling, indicate that FGF10 modulates the range of Wnt effects, likely via induction of *Sostdc1* expression. We suggest that modification of the reach of Wnt signaling could be due to local changes in morphogen diffusion, representing a novel mechanism in this tissue context, and we propose that this phenomenon might be involved in a broader array of mammalian developmental processes.

KEY WORDS: FGF, Wnt, Tongue, Taste papilla

INTRODUCTION

Taste is one of the fundamental senses in vertebrates and is crucial for discrimination between nutritious substances and potentially toxic ones. The basic taste structures of mammals consist of clusters of neuroepithelial receptor cells called taste buds. Although taste buds can be found at various locations within the oral cavity, including on the palate or epiglottis, most reside on the dorsal surface of the tongue. Taste buds are housed in highly organized structures called taste papillae. Three distinct types of gustatory papillae reside on the rodent tongue: small fungiform papillae are found on the anterior tongue, whereas the posterior tongue contains the larger foliate papillae and a single midline circumvallate papilla (CVP). Among members of a given species,

there is high intra-individual variability in the number of taste buds and in the number of taste cells within the taste bud in fungiform papillae; this is often connected to the terms 'supertaster' or 'nontaster' in humans (Bartoshuk et al., 1994; Miller and Reedy, 1990). Therefore, the number and size of the fungiform papillae are important for taste quality, and understanding the process of fungiform papillae patterning is required for determining how tastes are perceived.

The general rules of patterning of functional structures such as taste papillae or hair follicles are central aspects of developmental biology. Over the past few decades, research using rodent models has shown that the patterning and distribution of mature fungiform papillae is driven by specific cellular and molecular mechanisms that occur during prenatal tongue development (Chaudhari and Roper, 2010; Kapsimali and Barlow, 2013). This process starts at embryonic day (E) 12.5 in mouse by formation of epithelial thickenings called taste placodes. From E13.5 to E14.5, the placodes evaginate, forming raised structures called papillae. Around birth, taste bud cells differentiate within the mature papillae (Kaufman, 1992; Mistretta and Liu, 2006).

Canonical Wnt/β-catenin signaling has been identified as a positive effector of fungiform papillae development. *In vitro* treatment with LiCl, an activator of Wnt signaling via GSK3 inhibition, makes papillae both larger and more numerous, whereas overexpression of the Wnt antagonist *Dkk1* or inactivation of β-catenin cause a severe decrease or complete elimination of papillae (Liu et al., 2007). The Wnt ligand WNT10B has been proposed to play a major role in placode formation, and the fungiform papillae are reduced but not completely eliminated in *Wnt10b*-null mice (Iwatsuki et al., 2007). Another Wnt ligand reported to be expressed in tongue epithelium during the fungiform patterning period is WNT10A (Liu et al., 2007), and mutations in *Wnt10a* cause marked reduction of fungiform papillae in humans (Adaimy et al., 2007).

Whereas canonical Wnt signaling is known to induce the development of fungiform papillae, multiple pathways have been shown to inhibit their formation. One of the best studied of these is the SHH pathway. *Shh* expression lies downstream of Wnt signaling and was described to function in a negative-feedback loop with Wnt (Iwatsuki et al., 2007). SHH has both long- and short-range inhibitory effects on taste papillae, as blocking of SHH activity by cyclopamine, jervine or the anti-SHH 5E1 antibody leads to both larger and more numerous papillae (Hall et al., 2003; Iwatsuki et al., 2007; Liu et al., 2004). Despite these inhibitory effects during development, *Shh* expression also serves as a reliable and widely used marker of the fungiform placodes (Iwatsuki et al., 2007; Liu et al., 2004, 2013). SHH also plays an important role in the differentiation of taste cells. Lineage tracing experiments revealed that cells of taste placodes expressing *Shh* are taste cell progenitors, but do not contribute to the rest of the mature papilla epithelium, which forms later (Thirumangalathu et al., 2009). After E16 in rat

[1]Department of Orofacial Sciences and Program in Craniofacial Biology, University of California San Francisco, San Francisco, CA 94143, USA. [2]Institute of Molecular Genetics of the CAS, v. v. i., Czech Centre for Phenogenomics and Laboratory of Transgenic Models of Diseases, Division BIOCEV, Prumyslova 595, Vestec 252 42, Czech Republic. [3]Developmental Biology Program, Institute of Biotechnology, University of Helsinki, PO Box 56, Helsinki FIN-00014, Finland. [4]Stowers Institute for Medical Research, Kansas City, MO 64110, USA. [5]Department of Anatomy and Cell Biology, University of Kansas Medical Center, Kansas City, KS 66160, USA. [6]Department of Pediatrics and Institute for Human Genetics, University of California San Francisco, San Francisco, CA 94143, USA.

*Authors for correspondence (jernvall@fastmail.fm; ophir.klein@ucsf.edu)

M.P., 0000-0002-3773-8995; J.J., 0000-0001-6575-8486; O.D.K., 0000-0002-6254-7082

DEVELOPMENT

(corresponding to E14.5 in mouse), disturbances in SHH signaling can no longer affect the patterning of papillae (Liu et al., 2004) and Wnt activity is no longer restricted to the papillary epithelium; *Wnt10b* expression disappears at later developmental stages (Iwatsuki et al., 2007). These findings indicate that the period between E12.5 and E14.5 in mouse is crucial for fungiform papillae development and suggest that the primary patterning is completed by the end of this period. Beside its roles during embryonic development, SHH also plays a positive role in maintenance of adult papillae (Liu et al., 2013; Miura et al., 2001). In addition to SHH, other epithelial factors that inhibit fungiform papillae formation include BMP and EGF (Liu et al., 2008; Zhou et al., 2006). Despite the generally accepted importance of epithelial-mesenchymal interactions for development of budding epithelial structures such as teeth or hair (Ahn, 2015; Kettunen et al., 2000), little is known about the role of mesenchymal morphogens in papilla development. One exception is follistatin, a BMP inhibitor expressed in the mesenchyme, which affects the patterning and differentiation of fungiform papillae (Beites et al., 2009). In addition, the non-canonical *Wnt5a* expressed in the mesenchyme affects the overall size of the tongue, and exogenous WNT5A also inhibits papillae formation; nevertheless, neither the number nor size of fungiform papillae is altered in *Wnt5a*$^{-/-}$ tongues (Liu et al., 2012). Importantly, although SHH, BMP and EGF signaling are known to affect the number of the papillae, and some of these pathways also influence the size of the placodes, none of the factors affects the size of the papillae without changes in the papillary spacing and general patterning.

We have previously shown that the number of CVPs is regulated by a balance between sprouty (SPRY) genes and mesenchymally expressed *Fgf10*, which, respectively, antagonize and activate receptor tyrosine kinase (RTK) signaling (Petersen et al., 2011). Here, through analysis of the role of *Fgf10* in the patterning of fungiform papillae during embryonic development, we demonstrate that FGF signaling inhibits the size but does not affect the number of the fungiform papillae. This reveals that FGF10 has a unique role as a mesenchyme-derived inhibitor of fungiform papillae development. The effect of FGF signaling occurs post-transcriptionally, and we propose that local effects on Wnt diffusion regulate papillary size. Computational modeling based on our results showed that the process of diffusion can account for formation of phenotypes similar to those found in *Fgf10* and *Spry2* mutants. Our results further suggest a mechanism whereby changes in the extracellular matrix (ECM) environment can mediate alterations of Wnt ligand diffusion. Taken together, our analyses demonstrate that the FGF pathway has important regulatory input in fungiform papillae development and suggest this is mediated by a mechanism that modulates the range of ligand diffusion.

RESULTS
FGF signaling controls the fungiform progenitor field size
Fgf10 is expressed in tongue mesenchyme under the papillary field (Fig. 1A,A′) and signals to the epithelium, where *Spry2*, an RTK signaling antagonist, is expressed (Fig. 1B,B′). Therefore, mutations in these genes produce low and high levels of FGF signaling, respectively. We performed whole-mount *in situ* hybridization for *Shh*, a marker of fungiform papillae, in wild-type, *Fgf10*$^{-/-}$ and *Spry2*$^{-/-}$ tongues (Fig. 1C-E′) at E14.5, when patterning of the fungiform papillae can be readily analyzed. The taste papillae in *Fgf10*$^{-/-}$ embryos appeared larger than in wild type, whereas the papillae in *Spry2*$^{-/-}$ embryos were smaller than controls, which we confirmed by quantification of the size of

Shh-positive areas corresponding to papillae (Fig. 1F). In addition, the number of *Shh*-positive papillae in *Spry2*$^{-/-}$ tongues was lower than in controls, in contrast to *Fgf10*$^{-/-}$ tongues, which appeared to have a normal number of papillae (Fig. 1G). The decreased number of papillae, scored as visible *Shh*-positive areas in the *Spry2*$^{-/-}$ tongues, is likely attributable to the small size of the papillae, such that some become too small to visualize. These data suggest that the FGF pathway tunes the size of the papillary field but does not primarily influence the number and general pattern of the papillae. To confirm this idea, we quantified the inter-papillary spacing and found no significant differences between the genotypes (Fig. 1H), further indicating that the size but not the pattern of papillae is regulated by FGF signaling.

To investigate whether the differences observed at E14.5 (Fig. 1) were preserved in the already patterned but not yet mature taste papillae, we analyzed embryos at E18.5 (Fig. S1); this is the latest stage at which we can examine mature papillae in the *Fgf10*$^{-/-}$ mutants due to perinatal lethality. At this stage, the taste buds are not fully mature but do express taste cell and neuronal markers. We performed immunofluorescence staining on 10 μm frontal tongue sections using an antibody against cytokeratin 8 (KRT8), which marks all taste cell types, and by staining for the neuronal marker β-III tubulin (TUBB3) (Fig. S1A-I). The KRT8-positive cells were present within the presumptive taste buds of wild-type and FGF pathway mutants (Fig. S1A,D,G). TUBB3 expression in the *Fgf10*$^{-/-}$ and *Spry2*$^{-/-}$ taste buds was similar to wild type (Fig. S1B,E,H), indicating that these structures are innervated and likely functional.

We next quantified the average number of taste buds per section in different genotypes. We analyzed a region of the distal part of the tongue dorsum (excluding the tip), which is relatively uniformly covered with fungiform papillae; the analyzed area is shown in Fig. S1J. Additionally, by measuring taste bud diameter, we assessed the size of the taste buds, which reflects the number of taste cells. We found that the FGF pathway negatively regulates the size of presumptive taste buds: the taste buds in mutants lacking *Fgf10* were significantly larger than controls, whereas in *Spry2*$^{-/-}$ tongues, the taste bud size was diminished (Fig. S1Q). Furthermore, the number of taste buds was normal in *Fgf10*$^{-/-}$ mutants and decreased in the *Spry2*$^{-/-}$ mutants, similar to the earlier embryonic stage phenotypes (Fig. S1R). These data suggest that, by regulating the size of the fungiform progenitor field, FGF signaling determines the size of the future taste buds.

FGF signaling regulates canonical Wnt activity in developing papillae
Because canonical Wnt signaling is a key pathway in taste papilla patterning (Iwatsuki et al., 2007; Liu et al., 2007), we next investigated interactions between the Wnt and FGF signaling pathways in the developing tongue. We crossed both *Fgf10*- and *Spry2*-null mice with the BAT-gal reporter mouse, which expresses β-galactosidase in the presence of activated β-catenin and therefore indicates canonical Wnt signaling. This analysis found no evidence of Wnt activity during the initial fungiform papilla patterning process at E11.5. However, at ~E12.0, the Wnt signal starts to spread over the tongue dorsum and covers it, and, by E14.5, the pattern of future fungiform papillae positions is established (Fig. S2A-E). Frontal sections of X-gal-stained BAT-gal tongue at E12.5 show that Wnt/β-catenin activity is restricted to the epithelium and is absent from underlying mesenchyme in the fungiform papillary field, but Wnt/β-catenin activity is present in the mesenchyme under the papilla-free midline zone (Fig. S2F). This indicates that Wnt does not signal to the papillary field
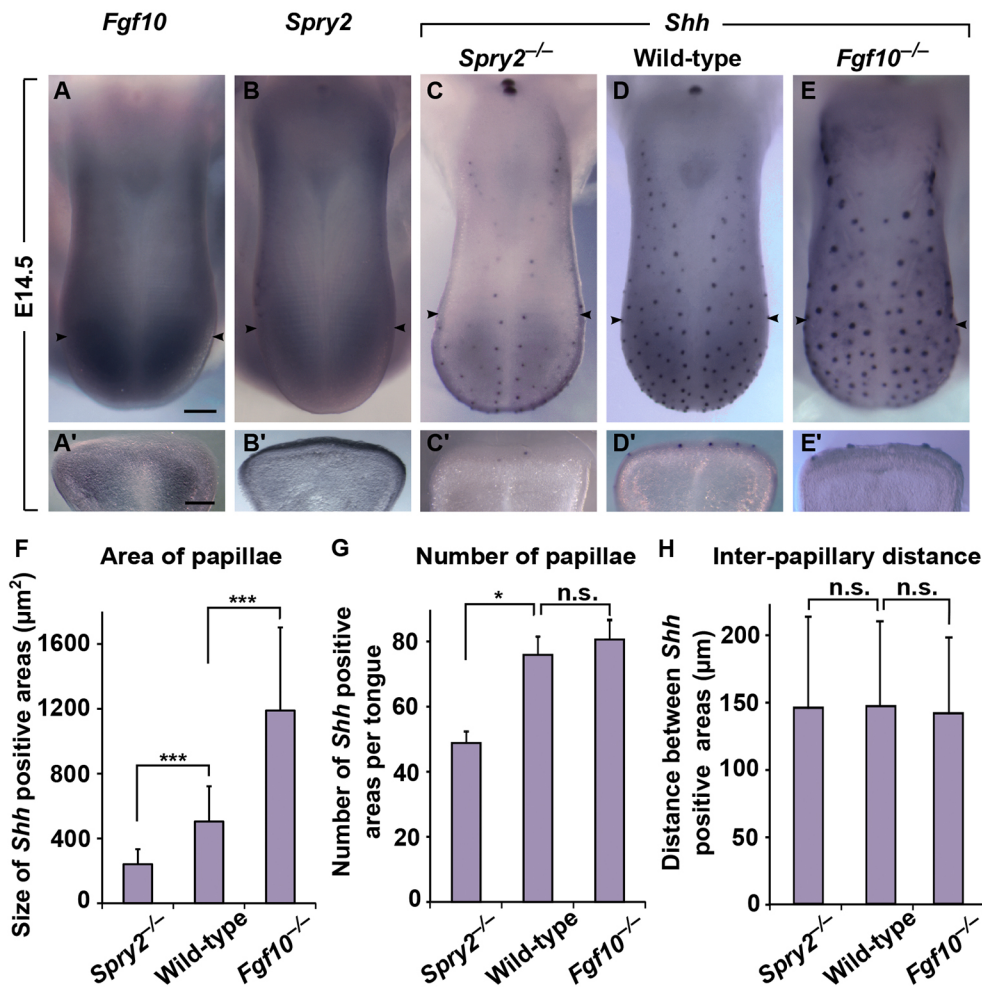
Fig. 1. FGF10 negatively regulates size of fungiform papillae during embryonic development. (A,B) *Fgf10* and *Spry2 in situ* hybridization at E14.5. (C-E) Opposite effects on fungiform papillae phenotype visualized by *Shh* whole-mount *in situ* hybridization at E14.5 can be observed in *Fgf10⁻/⁻* versus *Spry2⁻/⁻* mice in comparison with wild type. (A′-E′) Frontal vibratome sections (150 μm) of tongues (positions marked by arrowheads in A-E). (F-H) The evaluation of papillae number, size and distance in different genotypes. (F,H) *n*=5, (G) *n*=8. *P<0.05, ***P<0.0005, n.s., not significant. Scale bars: 250 μm.

mesenchyme expressing *Fgf10*, but it leaves the connection between Wnt and FGF signaling unresolved.

Examination of Wnt activity in mutants demonstrated genotype-specific differences. We examined the domain of Wnt/β-catenin activity at E14.5 (Fig. 2A-C′) and found that, in *Spry2⁻/⁻* tongues, the BAT-gal signal was also visible in the areas where no *Shh* signal was detected by *in situ* hybridization. This supports the notion that patterning is preserved in these mutants and that the apparent absence of some placodes is a reflection of their very small size (Fig. 2A). We also found that the signal in *Spry2⁻/⁻* tongues remained strong in the papillary areas but was largely absent from inter-papillary epithelium compared with the wild type. The focally robust BAT-gal signals in both the *Spry2⁻/⁻* and the wild-type papillae were in sharp contrast with the more diffuse, 'salt and pepper' pattern in *Fgf10⁻/⁻* papillae (Fig. 2A-C′; Fig. S2J-L in sections). The diffuse and focal BAT-gal signals in *Fgf10⁻/⁻* and *Spry2⁻/⁻* papillae, respectively, suggest that FGF signaling may regulate papilla size by inhibiting spreading of the Wnt signal.

We also examined the BAT-gal pattern at E12.5, when Wnt activity is in a dynamic phase. The domains of Wnt/β-catenin activity were enlarged in *Fgf10⁻/⁻* and reduced in *Spry2⁻/⁻* mutants (Fig. S2G-I). Despite these visual differences, the overall levels of *lacZ* expression in FGF mutant tongues positive for BAT-gal compared with the wild type appeared largely unaffected at both E12.5 and E14.5 (Fig. 2D, Fig. S2M), further supporting the hypothesis that spreading of the Wnt signal but not the overall level of signaling is controlled by FGF signaling.

RT-qPCR analyses of Wnt, FGF and SHH pathway components demonstrate a complex network of signaling interactions

Next, to examine the relationship between FGF and Wnt signaling at the transcriptional level, we performed *in vitro* culture followed by RT-qPCR analysis. Because of the well-studied role of *Shh* in fungiform development, we examined the relationship between SHH, Wnt and FGF pathways. Wild-type embryonic tongues dissected at E12.5 were cultured *in vitro* for 5 or 20 h with addition of LiCl (Wnt agonist), PNU74654 (Wnt antagonist), recombinant FGF10, SU5402 (FGF signaling antagonist), cyclopamine (SHH antagonist), SAG (SHH agonist) and compared with untreated controls (Fig. 3A). The cultured tongues analyzed after 5 and/or 20 h are shown in Fig. S3A; effects of treatments are qualitatively visualized by *in situ* hybridization for *Shh*.

First, we looked for evidence of auto-activation of the Wnt pathway in this system. Two Wnt ligands are expressed in the tongue epithelium, *Wnt10a* and *Wnt10b*, and the latter is considered to be the principal activating ligand in the tongue (Iwatsuki et al., 2007; Liu et al., 2007). We confirmed by whole-mount *in situ* hybridization that the expression of both genes during the period of fungiform development mirrored the placode pattern (Fig. S2N-P,S-U) as both ligands were expressed at low levels, with the *Wnt10b* signal appearing weaker and more restricted within the placodes. To localize the expression patterns in greater detail, we also performed *in situ* hybridization on frontal tongue sections. Whereas *Wnt10a* was expressed throughout the entire placode (Fig. S2V), *Wnt10b*
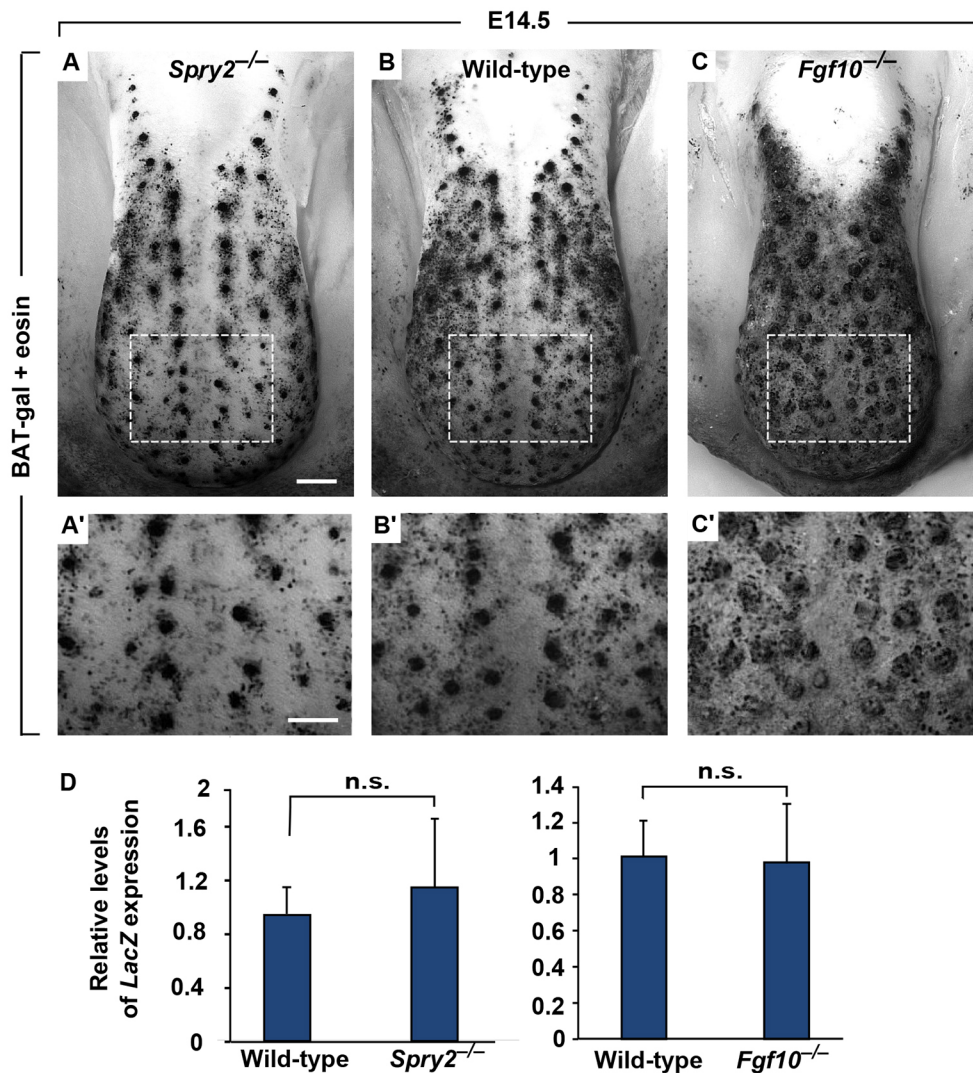
Fig. 2. The pattern but not the level of Wnt/β-catenin activity is altered in FGF pathway mutants. (A-C′) BAT-gal reporter mice crossed with $Fgf10^{-/-}$ and $Spry2^{-/-}$ mutants compared with wild type at E14.5 show the negative effect of FGF signaling on dispersion of Wnt activity outwardly from the taste placode center; Eosin counterstain was used to enhance the contrast. White boxes mark areas shown at higher magnification in A′-C′. (D) lacZ expression is not altered in BAT-gal-positive FGF pathway mutants (n=5). Scale bars: 250 µm in A-C; 150 µm in A′-C′.

expression was present only in the single central cell of each placode (Fig. S2Q,R), such that these two Wnt ligands have a nested distribution within the tongue epithelium. *Wnt10a* would appear to have a wider transcriptional range than *Wnt10b*, which has a single cell as its source. Nevertheless, the RT-qPCR data show that *Wnt10b* responds faster and more strongly to LiCl treatments than *Wnt10a*, supporting a role for *Wnt10b* as the principal autoregulatory activator during development of fungiform papillae (Fig. 3B,C). PNU74654 treatments downregulated both *Wnt10a* and *Wnt10b* after 20 h of treatment (Fig. 3G). Furthermore, *Dkk1* expression is upregulated in response to LiCl treatment (Fig. 3G), indicating that Wnt signaling negatively regulates itself in this context. However, PNU74654 treatments did not downregulate *Dkk1*, suggesting that other factors may also regulate *Dkk1*.

We further explored a potential link between FGF and Wnt signaling, and discovered that neither stimulation (using recombinant FGF10; rFGF10) nor inhibition (using SU5402) of FGF signaling caused a marked alteration in the expression levels of *Wnt10a* and *Wnt10b* (Fig. 3D,E,G). Moreover, while LiCl and PNU74654 treatment changed the expression of both the Wnt downstream target gene, *Axin2*, and the *lacZ* reporter in the BAT-gal mice as expected, neither the SU5402 nor rFGF10 treatment caused such changes (Fig. 3B-E,G). These data are in agreement

with those obtained from BAT-gal reporter mice crossed with $Fgf10^{-/-}$ and $Spry2^{-/-}$ mutants (Fig. 2D, Fig. S2J).

Of those that we tested, the only Wnt-related gene that exhibited marked changes in expression after SU5402 and rFGF10 treatment was *Sostdc1*, which was upregulated by FGF signaling after 5 h (Fig. 3F,G). SOSTDC1 is a secreted protein that is a putative Wnt inhibitor, but its precise function is unknown, and its effects appear to be context dependent (Guidato and Itasaki, 2007; Itasaki et al., 2003; Kassai et al., 2005; Lintern et al., 2009; Ohazama et al., 2008). During the period of fungiform papillae development, *Sostdc1* expression uniformly covers the papillary field on the tongue dorsum (corresponding to the pattern of *Fgf10* expression, Fig. 1A,A′; Fig. S3K,L), as can be seen in whole-mount hybridized tongues (Fig. S3B-D). *Sostdc1* expression localizes to the border of the mesenchyme and epithelium, as seen in frontal tongue sections (Fig. S3E-J). Notably, at E13.5 and E14.5, when the epithelium is multilayered, the cells closer to the mesenchyme are positive, but the superficial layer cells do not express the *Sostdc1* (Fig. S3I,J). In the developing tongue, *Sostdc1* has been reported to inhibit fungiform papilla development (Ahn et al., 2010), which we confirmed by whole-mount *in situ* hybridization of tongues from embryos overexpressing *Sostdc1* in the lingual epithelium (K14-tTA;tetO-Wise, Fig. S3M). In agreement with the SU5402 and rFGF10 treatments, and with the K14-tTA;tetO-Wise (*Sostdc1* OE)
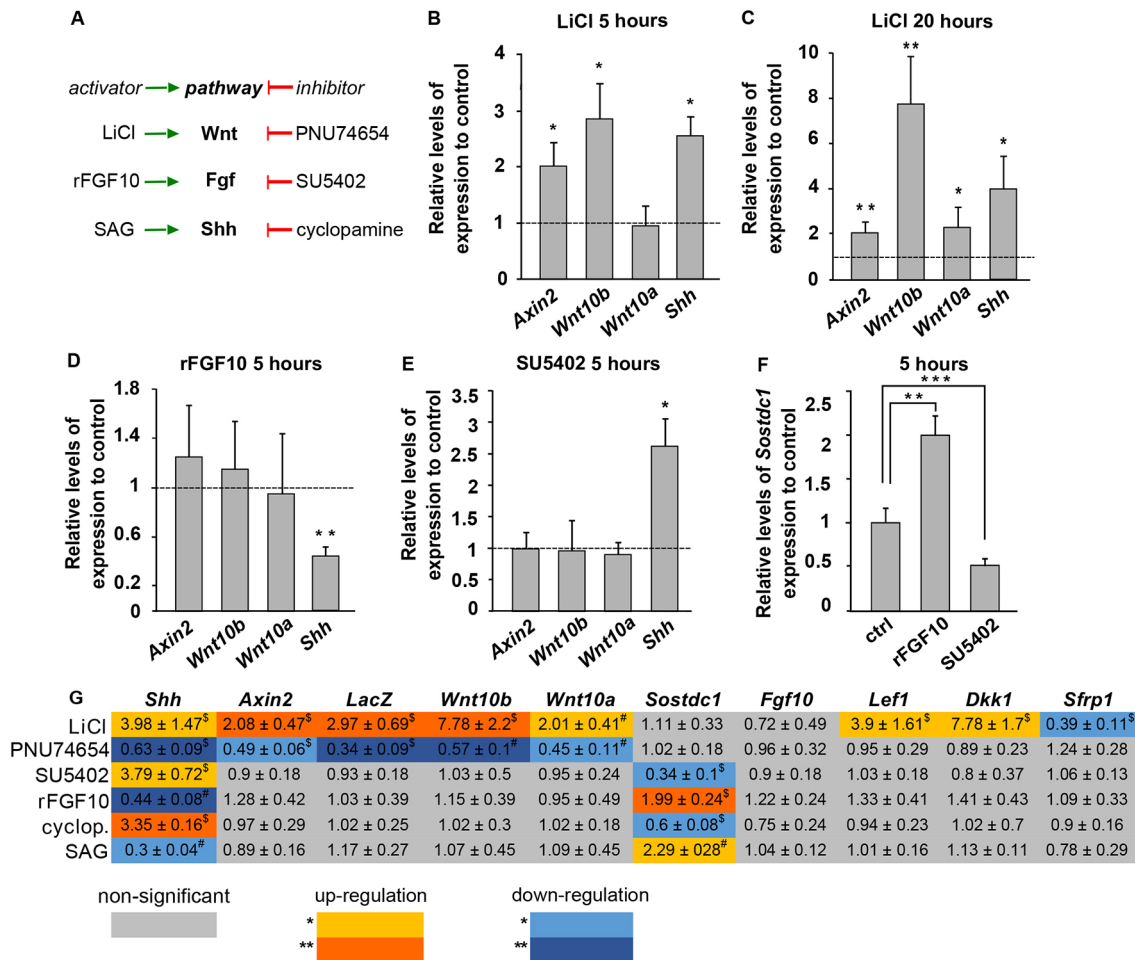
Fig. 3. RT-qPCR analyses of Wnt, FGF and SHH pathway interactions. (A) Summary of the actions of small bioactive molecules and chemicals used for *in vitro* culture treatment. (B-F) RT-qPCR analysis of changes in gene expression in tongue explant cultures treated with LiCl, SU5402 and rFGF10 compared with untreated control samples (fold ratio). (G) Summary table of complete RT-qPCR results for different treatments compared with control (5 h of treatment with rFGF10, and 20 h of treatment with LiCl, PNU74654, SU5402, cyclopamine and SAG). Values are mean fold ratio±s.d. (B,C,E,F) *$P<0.025$, **$P<0.0025$, ***$P<0.00025$; (D) **$P<0.005$; (G) #/*$P<0.025$, #/**$P<0.0025$; $/*$P<0.05$, $/**$P<0.005$. Data represent mean values±s.d. See Table S6 for a list of n, P and F values, and degrees of freedom for B-G.

embryos, *Sostdc1* expression was downregulated in *Fgf10*^{−/−} tongues and upregulated in *Spry2*^{−/−} tongues (Fig. S3N). These results suggest that FGF signaling inhibits Wnt signaling and fungiform papillae formation through SOSTDC1. Such inhibitory effects of FGF10 and SOSTDC1 on Wnt signaling would likely be indirect, because RT-qPCR analysis of *Sostdc1* OE tongues showed that, similar to SU5402 and rFGF10 treatment, expression of *Axin2*, *Wnt10b* and *Wnt10a* were largely unaffected (Fig. S3O).

In addition to Wnt and FGF pathway activity, we also tested the effect of modulation of SHH signaling and responses at the level of *Shh* expression after different treatments. Consistent with published data (Iwatsuki et al., 2007), our transcriptional analysis showed that *Shh* is upregulated by Wnt signaling (Fig. 3G). Nevertheless, neither activation nor inhibition of the SHH pathway by SAG or cyclopamine, respectively, caused significant changes in *Wnt10a*, *Wnt10b*, *Axin2* or *lacZ* expression (Fig. 3G). Thus, these experiments did not indicate direct feedback inhibition of the Wnt pathway by SHH signaling in the tongue. We next tested potential interactions that could result in *Fgf10* activation or inhibition using transcriptional analyses. As we did not observe any significant changes after any of the treatments (Fig. 3G), *Fgf10* is likely not activated or inhibited by Wnt and SHH signaling, or by FGF10 itself.

Computational modeling of fungiform papillae patterning

To further investigate the plausibility of different hypotheses regarding the role of FGF signaling, we implemented a simple reaction-diffusion model to simulate the papilla patterning process. As a starting point to set our model dynamics, we used the network based on our experimental data (Fig. 4B,C). The activator in the model is Wnt, representing the combined effect of WNT10B and WNT10A, and it is auto-activated. Even though SHH has been suggested as a potential inhibitor (Hall et al., 2003; Iwatsuki et al., 2007; Liu et al., 2004), our data do not support direct links to Wnt inhibition at the transcriptional level, and, therefore, we assumed DKK1 to be a classical inhibitor to Wnt in our system (upregulated by LiCl, Fig. 3G). We removed SHH from the system altogether, because there is no feedback regulation of Wnt or FGF10 by SHH (Fig. 4A). This network, which essentially has the classical activator-inhibitor dynamic, was implemented using Gierer-Meinhardt reaction kinetics to describe the interaction of the activator and the inhibitor. Because the BAT-gal data suggested that FGF signaling inhibits the spreading of Wnt/β-catenin activity (Fig. 2A-C′), we extended the classical model by a local diffusion inhibition mechanism for the activator (see supplementary Materials and Methods). We considered FGF10 to have a uniform
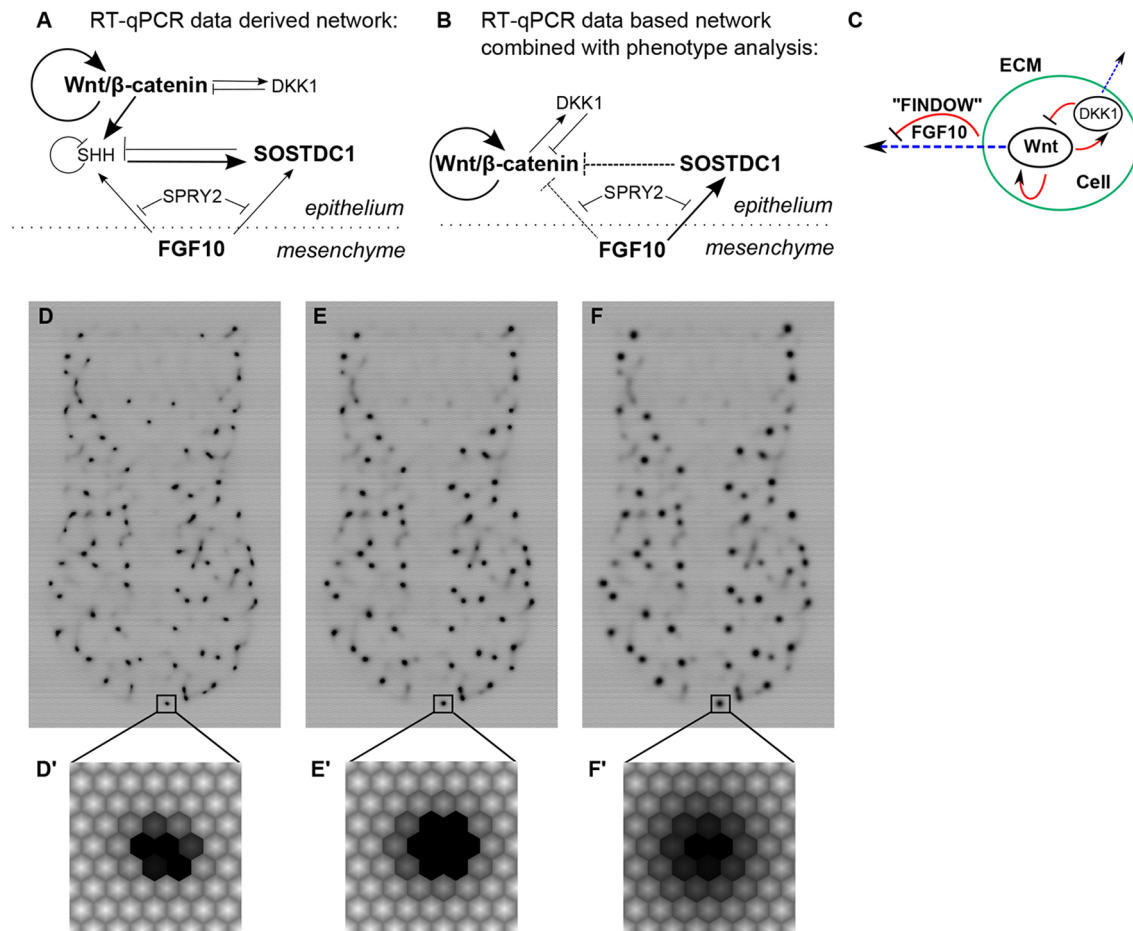
Fig. 4. Computational modeling input and results. (A) Model network derived solely from RT-qPCR data. (B) Adjusted model network combining RT-qPCR and data gained by phenotyping FGF pathway mutants. (C) Simplified schematic of network shown in B used as a base for computational modeling with FINDOW parameter. Dashed arrows suggest a non-transcriptional effect. (D-F) Results of different levels of the FINDOW parameter (D=2.0; E=0.2; F=0.0) resemble the FGF pathway mutant phenotypes: from dense signal in a small area in D (similar to $Spry2^{-/-}$ tongues) to diffuse signal in a larger area in F (similar to $Fgf10^{-/-}$ tongues) with no primary effect on the number of papillae. (D′-F′) Detailed images of the papillary field.

source in the underlying mesenchyme and, further, that FGF10 does not interact with the epithelial morphogens in ways that cause significant changes in its concentration. Consequently, we reduced FGF10 to a constant multiplier, which we dubbed as FINDOW (FGF inhibiting diffusion of Wnt). The action of SOSTDC1 is implemented within the FINDOW function.

Our model further differs from classical reaction diffusion models in that we incorporated a cellular differentiation mechanism, whereby the source terms in the model equations undergo changes as a result of computational nodes (i.e. cells) that reach threshold morphogen levels (for a full list of reaction-diffusion parameters see Table S1). The main reason for including the differentiation mechanism was to obtain a realistic depiction of development, which also preserves the observed noisiness of the papillae patterning. As a consequence, our model readout is not a morphogen concentration level but a differentiation level describing the transition of nodes to papillary nodes (for a full list of differentiation parameters see Table S2). To minimize the complexity of our model, we assumed that the effects of tissue growth on patterning are negligible, and that the physical presence of the mesenchyme can be ignored, thus reducing the model into a 2D fixed-domain simulation. To both curtail the grid effects and to best capture the average epithelial cell shapes under optimal spatial packing, the spatial discretization scheme used was a hexagonal grid

(Fig. S4A,B). To facilitate the comparison between the simulation output and the real patterns, we set the model domain to resemble the tongue shape (Fig. S4C). For further details and discussion on the model implementation, see supplementary Materials and Methods.

To validate our model, we systematically explored whether any of the 'classical' activator-inhibitor parameters, excluding FINDOW, could account for the observed $Fgf10$ and $Spry2$ mutant phenotypes (Fig. S4D). We found that all the classical parameters tended to affect both the papilla size and the wavelength in unison, thereby causing more extensive changes in the papillae than the size-specific effects of $Fgf10$ and $Spry2$ found in our experiments. By contrast, changing the value of FINDOW within a reasonable range maintained the patterning wavelength intact while changing papilla size. In comparison with medium (wild-type) value (Fig. 4E), low values of the FINDOW parameter produced large and diffuse activator fields, resulting in larger papillae similar to the $Fgf10^{-/-}$ mutant (Fig. 4F), whereas high FINDOW parameter values produced small and concentrated papillary fields similar to $Spry2^{-/-}$ embryos (Fig. 4D). The detailed images of the papillary field (Fig. 4D′,E′,F′; Fig. S4F) show the different range of activator diffusion negatively correlated with the level of the activator within one cell. Moreover, the number of papillae and the wavelength of the pattern resulting in inter-papillary spacing is not primarily

affected in this model, which is consistent with our analysis of the mutant phenotypes.

In summary, we found that the FINDOW model is capable of producing the changes in papilla size while keeping the patterning wavelength intact, thus supporting the hypothesis that changes in diffusion can lead to patterning phenotypes observed in $Fgf10^{-/-}$ and $Spry2^{-/-}$ papillae.

The ECM environment and Wnt diffusion

Our experiments and modeling indicate that the network regulating papilla size may not operate exclusively at the level of gene expression. Therefore, we set out to examine the distribution of SOSTDC1, the Wnt-related protein that showed differences at the transcriptional level in response to changes in FGF signaling. We performed whole-mount SOSTDC1 immunofluorescence staining of tongue epithelium. The staining was concordant with the gene expression data and showed that, at E12.5, the $Fgf10^{-/-}$ tongue epithelium (Fig. 5E,F) contains very low levels of SOSTDC1 compared with wild type (Fig. 5A,B). At E14.5, similar staining was observed but with high local peaks of SOSTDC1 in the control that were not present in the $Fgf10^{-/-}$ tongues (Fig. 5C,D,G,H).

Secreted SOSTDC1 protein has been suggested to bind heparan sulphate proteoglycans (Lintern et al., 2009), and we next addressed the more general question of whether disruption of extracellular matrix (ECM) glycosaminoglycans using heparinase could cause spreading of Wnt activity. E12.5 BAT-gal-positive embryos were harvested and cultured in liquid medium for 2 h with or without heparinase and then transferred at the surface of semisolid medium and incubated for an additional 20 h. The heparinase treatment resulted in a more diffuse pattern of Wnt activity compared with untreated samples (Fig. 5I-K). Moreover, a similar effect was observed when we treated tongues from $Spry2^{-/-}$ embryos with heparinase, including a significant increase in the size of the BAT-gal area compared with untreated $Spry2^{-/-}$ tongues (Fig. S5A-C). Heparinase treatment appears to rescue the papillae development in $Spry2^{-/-}$ tongues, indicating that the extracellular environment can affect diffusion of the Wnt signal in the tongue.

DISCUSSION

Understanding the complex interactions between morphogenetic pathways is a principal goal of modern developmental biology. The classical view of the actions of morphogens such as FGF10 or Wnt is based on the assumption that they function within gene regulatory networks by affecting other players transcriptionally. However, it has been shown that some pathways, such as canonical Wnt signaling, can exploit different diffusion rates alone to form distinct patterns. Importantly, most of this work has been carried out in invertebrates such as *Drosophila* or butterfly (Monteiro et al., 2001; Yan and Lin, 2009), but relatively little has been performed in vertebrates.

Here, we present evidence regarding the negative effect of FGF10 on the size of fungiform papillae in mouse, and we argue that this action is not executed at the transcriptional level. Our phenotypic evidence is based on FGF signaling principally affecting size but not spacing of taste papillae (Fig. 1), an effect not readily produced by changing the standard reaction-diffusion parameters (Fig. S4D). Interestingly, the effect of FGFs in fungiform papillae is opposite to the phenotype we described in the circumvallate papilla (Petersen et al., 2011), where the level of $Fgf10$ was positively correlated to the size of the papillary field. This difference might result from different developmental origin (Rothova et al., 2012) and demonstrates the contextual complexity of developmental processes. In contrast to other morphogens described to affect

fungiform development, which affect both the spacing and number of papillae, mesenchymal FGF10 seems to play a very specific role in fine-tuning the pattern by affecting solely the size of the papillary area. Observed differences of Wnt-positive areas in BAT-gal tongues were reflected in changes of Shh expression. Interestingly, in $Spry2$ mutants there seems to be a minimal Wnt field size limit to trigger Shh expression. Therefore, as it was shown that the Shh expression is the marker of future taste cells (Thirumangalathu et al., 2009), this suggests the presence of more taste cells and fewer or no taste cells in the future papillae in $Fgf10^{-/-}$ and $Spry2^{-/-}$ tongues, respectively. This connection was supported by our observation of larger presumptive taste buds in $Fgf10$ mutant tongues and smaller taste buds, which were also lower in number, in $Spry2$ mutant tongues. These observations indicate that the FGF pathway perhaps affects the sensitivity of papillae to different tastes.

Our data further suggest that papilla size differences could be achieved by regulation of the spatial reach of Wnt effects, possibly by altering diffusion. We have identified a secreted protein, SOSTDC1, as a candidate for this action. However, the precise mechanism by which SOSTDC1 alters Wnt diffusion remains to be elucidated. SOSTDC1 has been described in various contexts to act as an inhibitor or as an activator of Wnt signaling (Itasaki et al., 2003); the possibility of its action at the level of diffusion might help to explain these contradictory results. Interestingly, SOSTDC1 binds both the Wnt co-receptor LRP6 and the negative regulator of Wnt signaling LRP4 (Lintern et al., 2009; Ohazama et al., 2008). During the development of fungiform papillae, the interaction of SOSTDC1 with one or both of these molecules may change the dynamics of Wnt ligand binding and subsequently affect further diffusion of the ligands. Another explanation could be that binding of SOSTDC1 to LRP4 and/or LRP6 hampers the accessibility of the receptors without changes in ligand diffusion; however, in this case effects downstream of the Wnt pathway should occur and these were not observed in our RT-qPCR analysis.

Our heparinase treatment experiments point to the importance of changes in ECM in general. The observed upregulation of $Sostdc1$ expression in response to FGF stimulation might be direct but could also be a secondary result of the structural changes in the ECM, because FGF receptors are known to be functionally connected to heparan sulfates (Mohammadi et al., 2005). Although the fact that $Sostdc1$ transcription is affected by FGF10 by 5 h after treatment *in vitro* points to direct downstream activation, SOSTDC1 might be part of a larger complex containing multiple ECM molecules, or there could be other proteins affected in parallel by FGF signaling. Even though we did not find a transcriptional connection, SFRP proteins are possible candidates to be involved in the changes of ECM environment triggered by FGF10, because of their known role as secreted Wnt antagonists (Kawano, 2003). Although the details of this process remain to be investigated in the future, the data reported here have identified a clear transcriptional connection between FGF10 and $Sostdc1$ both *in vitro* and in FGF pathway mutants, and this notion is supported by the uniform pattern of $Sostdc1$ expression above $Fgf10$-positive mesenchyme.

We made some intriguing observations related to timing in our *in vitro* experiments that will merit further study. The rFGF10 treatment caused transcriptional responses after 5 h, but these were no longer detectable after 20 h, likely due to compensation. Therefore, we focused on the transcriptional changes after 5 h of treatment with rFGF10. Additionally, we found that the effects of cyclopamine and SAG could be observed after 20 h but not after 5 h of treatment, indicating a delay in SHH action compared with other morphogens in the system. The effects of bioactive molecules
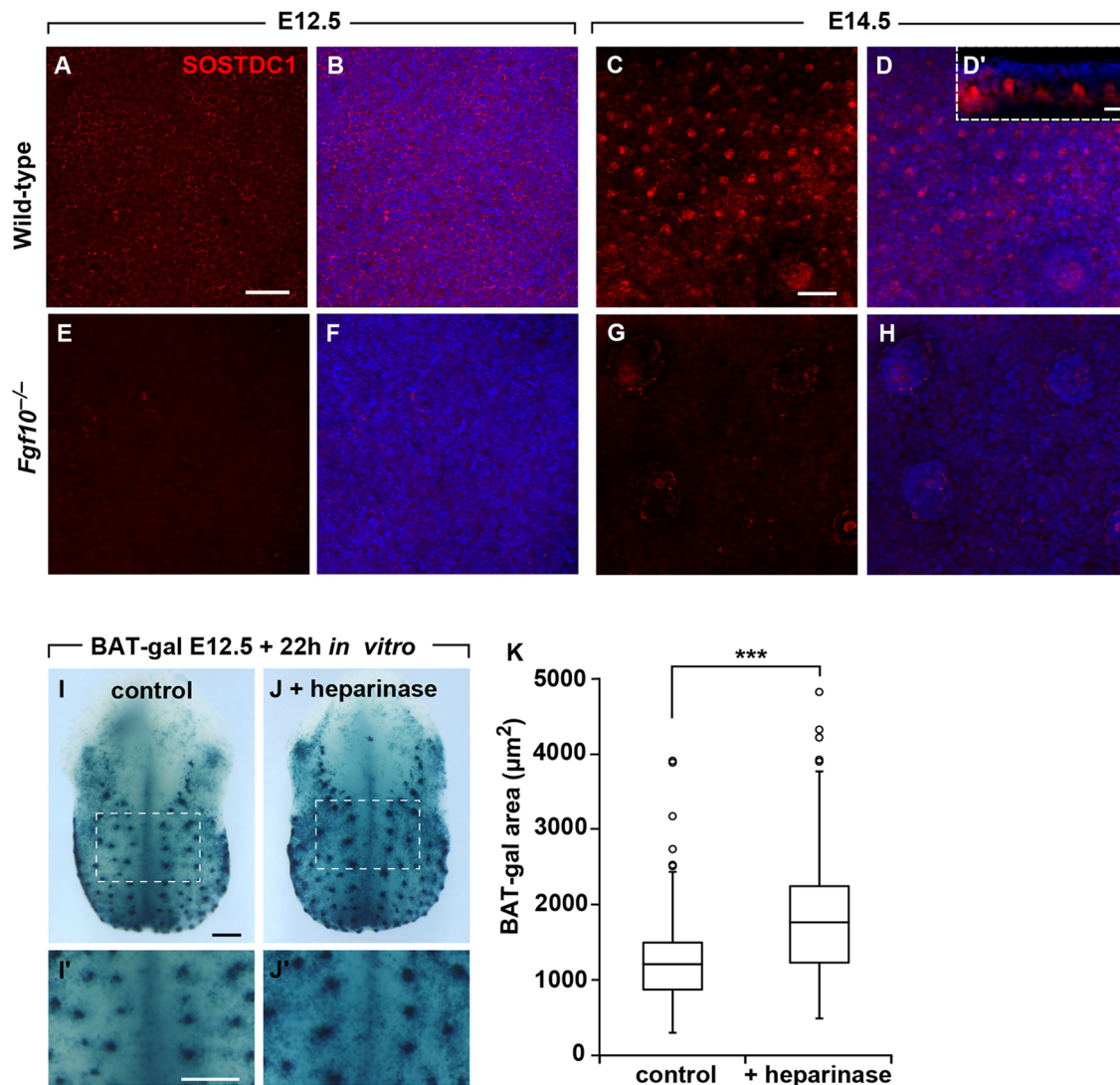
Fig. 5. The ECM environment and Wnt diffusion. (A-H) The FGF pathway affects the distribution of the secreted Wnt antagonist protein SOSTDC1. View of the dorsal tongue epithelium surface in whole-mount: the *Fgf10⁻/⁻* tongue epithelium contains a very low level of the SOSTDC1 protein compared with wild type at both E12.5 and E14.5. (D′) Frontal view of SOSTDC1 pattern from D, counterstained with DAPI (blue). (I-K) Wnt diffusion is affected by release of the ECM complexes by heparinase treatment. (I,J) E12.5 X-gal-stained tongue explants from BAT-gal littermates cultured *in vitro* with (J) or without (I) addition of heparinase. Heparinase-treated tongue (J) displays a more diffuse pattern of Wnt activity; white boxes mark areas shown at higher magnification in I′,J′. (K) BAT-gal-positive areas in control versus heparinase-treated littermate tongues (*n*=3). Boxes show the median and the interquartile range (IQR), ends of the whisker are set at 1.5 × IQR above the third quartile (Q3) and 1.5 × IQR below the first quartile (Q1) and circles represent the outliers. ***P<0.0005. Scale bars: 50 µm in A-H; 250 µm in I-J′.

applied for both culture time periods were similar after 5 and 20 h of treatment (see Fig. 3B-G).

In addition, our study highlights that the mechanism of SHH action in the patterning of fungiform placodes requires further investigation and should be considered in terms of non-transcriptional effects. The notion that the SHH inhibitory effect over Wnt occurred transcriptionally is based on comparison of expression of TOPGAL, a transgenic reporter similar to BAT-gal (Iwatsuki et al., 2007). As the changes in *Shh* expression after FGF signaling alterations cannot be explained by changes in Wnt signaling, the RT-qPCR results would suggest direct inhibition of *Shh* by the FGF pathway (as shown in Fig. 4A). However, if FGF10 inhibits *Shh*, a proven inhibitor of fungiform placode development, then FGF10 should act as an activator in the system, which is not consistent with mutant phenotypes we identified. Therefore, the changes in *Shh* expression under altered FGF signaling conditions appear to result from changes in the Wnt signaling field size. In other words, the transcriptional

changes and also the altered size of *Shh* expression domains observed in *Fgf10⁻/⁻* and *Spry2⁻/⁻* mutant tongues (Fig. 1) are likely caused by a higher or lower number, respectively, of cells reached by Wnt that trigger *Shh* expression. We also observed that *Shh* expression was downregulated in the *Sostdc1* OE tongues (Fig. S3M,O), which can be explained by prevention of Wnt signaling from spreading and, therefore, decreasing the activation of *Shh*. Moreover, similar to FGF10, we observe that SHH also activates the transcription of *Sostdc1 in vitro* (Fig. 3G). Interestingly, the *Sostdc1* expression does not seem to be enriched in the *Shh*-positive placodes, although this may be masked by the high level of *Sostdc1* in the inter-placode epithelium triggered by FGF10. These observations underscore the need for more-detailed investigation of the role of SHH in the process of tongue development. The non-transcriptional relationship between SHH and Wnt signaling involving SOSTDC1 is suggested in the alternative network in Fig. 4B. Furthermore, our computational modeling provides additional support for the non-transcriptional

regulation of papilla size or, at the very least, does not support the typical activator-inhibitor parameters (Fig. 4, Fig. S4D).

The data reported here suggest a potentially novel mechanism for regulation of fungiform papillae development by regulating diffusion of a ligand, in contrast to distinct mechanisms proposed with other pathways. For example, Bmp and Noggin (Zhou et al., 2006) or EGF (Liu et al., 2008) signaling have been proposed to maintain a balance between papillary and inter-papillary epithelium by inhibition of papillary cell fate via transcriptional influence on surrounding tissue. Taken together, we describe a novel inhibitory role of the FGF pathway during the patterning of fungiform papillae. We showed that FGF10 affects the area of Wnt activity, resulting in changes in the size of future fungiform papillae without altering the general pattern of the papillae. This regulation occurs post-transcriptionally, likely via changes in Wnt diffusion through ECM, and we suggest that such a mechanism might be involved in a much wider spectrum of mammalian developmental processes.

MATERIALS AND METHODS

Animals
Fgf10-null, *Spry2*-null and BAT-gal mice have been described previously (Maretto et al., 2003; Min et al., 1998; Shim et al., 2005). To obtain K14-tTA; tetO-Wise (Ahn et al., 2013) embryos, K14-tTA mice were mated with tetO-Wise (Tet-Off system) mice in the absence of doxycycline. In the double transgenic embryos, *Sostdc1* was overexpressed under the control of the K14 promoter. For detailed information about all mouse strains, see Table S3A,B. The protocol was approved by the UCSF Institutional Animal Care and Use Committee (Protocol Number AN084146). Mice were mated overnight, and the presence of a vaginal plug indicated embryonic day (E) 0.5. The harvested embryos were standardized by body weight (Peterka et al., 2002), and over- or underdeveloped embryos/litters were not analyzed. For details about numbers of analyzed litters/embryos, see Table S4; for details about the definition of structures analyzed by additional described methods see Table S5.

RNA *in situ* hybridization
Digoxygenin-labeled RNA probes (DIG RNA labeling kit, Roche) were generated by *in vitro* transcription from plasmids containing fragments of murine *Shh*, *Fgf10*, *Spry2* and *Sostdc1* or from PCR-amplified fragments of *Wnt10a* and *Wnt10b*. *In situ* hybridization was performed according to standard protocols (Wilkinson and Nieto, 1993) on tongues from E12.5 to E14.5 time periods after fixation in 4% PFA in whole mount or in 7 μm paraffin sections. Results of phenotype analysis are presented as an average± standard deviation. We analyzed the papillae on the dorsal surface of the tongue, and the measurements were performed in ImageJ 1.48v software. Kruskal-Wallis one-way analysis of variance was used for statistical evaluation of the papillae number. Analysis of variances was used for comparing differences among the three genotypes (inter-papillary distances and size). For the details of the analysis and statistical evaluation, see supplementary Materials and Methods; for the p, H and F values with degrees of freedom, see Table S6.

Whole-mount *lacZ* staining
Tongue tissues dissected from transgenic embryos, alternatively after being cultured *in vitro*, were fixed O/N in Mirsky's fixative (National Diagnostics), stained in X-gal solution and post-fixed in 4% PFA. In BAT-gal-positive tongues at E14.5, Eosin counterstain was used to enhance the contrast and the pictures were obtained using a fluorescence microscope (presence of β-gal quenches the natural fluorescence of Eosin in the red channel). Alternatively, the stained tongues were embedded in paraffin wax and sectioned at 7 μm.

Microscopy
Bright-field and fluorescent wide-field images were taken using a Leica DM5000B (*in situ* hybridization, *lacZ* and immunohistochemistry on sections). For confocal imaging, a Leica SP5 Confocal (whole-mount immunohistochemistry) was used. Images of whole-mount *lacZ*-positive tongues, hybridized tongues and vibratome sections were taken using Leica MZ16F stereomicroscope.

Immunohistochemistry
Immunohistochemistry was performed on 10 μm frozen sections according to standard protocol. Rat anti-cytokeratin 8 (TROMA-I, DSHB/deposited by P. Brulet and R. Kemler, Institut Pasteur, Paris; 5 μg/ ml) and mouse anti-β3 tubulin (MAB1195, R&D Systems; 5 μg/ml) were applied followed by incubation in anti-rat AlexaFluor 488 and anti-mouse AlexaFluor 555 secondary antibodies (Invitrogen). For evaluation of presumptive taste buds marked by KRT8, we analyzed 30 frontal frozen sections from the distal part of the tongue dorsum (marked in Fig. S1J). To compare the number of taste buds, we quantified the average number of taste buds per section. To assess the size, we measured average taste bud diameter using ImageJ 1.48v software. Results are presented as an average±standard deviation. Kruskal-Wallis one-way analysis of variance was used for statistical evaluation of the taste bud number. Analysis of variances was used for analysis of taste bud diameter. For details of the analysis and statistical evaluation, see supplementary Materials and Methods. Immunohistochemistry of whole-mount tongues was performed according to an Abcam protocol. Rabbit anti-SOSTDC1 (ab99340, Abcam; 5 μg/ml) was applied followed by incubation with anti-rabbit AlexaFluor 555 secondary antibody (Invitrogen).

Reverse transcription quantitative PCR
Isolated RNA was used as a template for reverse transcription into cDNA using a Reverse Transcription System (Promega). RT-qPCR (reverse transcription quantitative PCR) reactions were performed using the GoTaq qPCR Master Mix (Promega) in Mastercycler Realplex (Eppendorf). Expression levels of the genes of interest were normalized to levels of *Rpl19* and are presented as levels relative to wild type (set as 1). PrimeTime Primers purchased from IDT (Integrated DNA Technologies) were used in RT-qPCR reactions and primer sequences are available upon request. All experiments were performed independently in triplicate on at least three different specimens ($n{\geq}3$) per group. Data were analyzed with the $2^{-\Delta\Delta Ct}$ method and are presented as an average±standard deviation. The Mann-Whitney *U*-test was used to determine the *P*-value. In cases where two treatment groups were compared with one control group the Bonferroni correction of the *P*-level was applied. For all *P*, U and Z values with degrees of freedom, see Table S6.

Vibratome sections
The hybridized samples were embedded in 15% gelatin (300 Bloom)/PBS. The samples were cut in a series of 150 μm frontal sections using the Leica VT1000 S vibrating blade microtome (Leica Microsystems).

In vitro organ culture
Embryonic tongues carrying the BAT-gal allele were dissected at E12.5 and cultured at 37°C at the surface of semisolid 0.3% LMP agarose medium (Hu et al., 2005) for short (5 h) or long (20 h) time periods. Concentrations of bioactive molecules dissolved in medium were: 25 mM LiCl (Sigma-Aldrich, 203637), 30 μM PNU74654 (Sigma-Aldrich, P0052), 375 ng/ml of recombinant FGF10 protein (Abcam, ab191785), 2.5 μM SU5402 (Sigma-Aldrich, SML0443), 5 μM cyclopamine (Sigma-Aldrich, C4416) and 1 mM SAG (Smoothened agonist; Sigma-Aldrich, SML1314). For drugs diluted in DMSO, a corresponding concentration of DMSO was added to the control medium (in the case of two treatments compared with one control group, the higher of the concentrations was used). After incubation, the tongue explants were stabilized in RNAlater (Ambion). RNA was extracted using the RNeasy Mini kit (Qiagen) and DNA was removed in-column with RNase-free DNase (Qiagen). Alternatively, E12.5 BAT-gal-positive tongue explants were cultured 2 h *in vitro* in fluid tissue culture medium with or without added two Sigma units of heparinase III (Sigma-Aldrich, H8891). Subsequently, the explants were transferred at the surface agarose-containing medium and incubated for additional 20 h at 37°C. The tongue explants were then fixed

in Mirsky's fixative and X-gal stained. The measurements were performed using ImageJ 1.48v software, and analysis of variance was used for comparing differences among treated and untreated samples. For statistical analysis details, see supplementary Materials and Methods.

Computational modeling

The computational model was implemented in the C++ language. For technical details on the implementation, see supplementary Materials and Methods. The simulation source code and a graphical user interface (shown in Fig. S6) for running the simulation is available for download at http://dead.cthulhu.fi/MorphoMaker/.

Competing interests
The authors declare no competing or financial interests.

Author contributions
Conceptualization: M.P., J.P., J.J., O.D.K.; Methodology: M.P., T.J.H., J.P., A.H.J., J.J., O.D.K.; Software: T.J.H.; Validation: M.P., T.J.H., F.S.; Formal analysis: M.P., T.J.H., F.S.; Investigation: M.P.; Resources: Y.A., R.K., J.J., O.D.K.; Data curation: T.J.H.; Writing - original draft: M.P., T.J.H., J.J., O.D.K.; Writing - review & editing: J.P., F.S., A.H.J., R.K.; Visualization: M.P., T.J.H.; Supervision: J.P., J.J., O.D.K.; Project administration: J.J., O.D.K.; Funding acquisition: J.J., O.D.K.

Supplementary information
Supplementary information available online at
http://dev.biologists.org/lookup/doi/10.1242/dev.148080.supplemental

References
Adaimy, L., Chouery, E., Mégarbané, H., Mroueh, S., Delague, V., Nicolas, E., Belguith, H., de Mazancourt, P. and Mégarbané, A. (2007). Mutation in WNT10A is associated with an autosomal recessive ectodermal dysplasia: the odonto-onycho-dermal dysplasia. *Am. J. Hum. Genet.* **81**, 821-828.

Ahn, Y. (2015). Signaling in tooth, hair, and mammary placodes. *Curr. Top. Dev. Biol.* **111**, 421-459.

Ahn, Y., Sanderson, B. W., Klein, O. D. and Krumlauf, R. (2010). Inhibition of Wnt signaling by Wise (Sostdc1) and negative feedback from Shh controls tooth number and patterning. *Development* **137**, 3221-3231.

Ahn, Y., Sims, C., Logue, J. M., Weatherbee, S. D. and Krumlauf, R. (2013). Lrp4 and Wise interplay controls the formation and patterning of mammary and other skin appendage placodes by modulating Wnt signaling. *Development* **140**, 583-593.

Bartoshuk, L. M., Duffy, V. B. and Miller, I. J. (1994). PTC/PROP tasting: anatomy, psychophysics, and sex effects. *Physiol. Behav.* **56**, 1165-1171.

Beites, C. L., Hollenbeck, P. L. W., Kim, J., Lovell-Badge, R., Lander, A. D. and Calof, A. L. (2009). Follistatin modulates a BMP autoregulatory loop to control the size and patterning of sensory domains in the developing tongue. *Development* **136**, 2187-2197.

Chaudhari, N. and Roper, S. D. (2010). The cell biology of taste. *J. Cell Biol.* **190**, 285-296.

Guidato, S. and Itasaki, N. (2007). Wise retained in the endoplasmic reticulum inhibits Wnt signaling by reducing cell surface LRP6. *Dev. Biol.* **310**, 250-263.

Hall, J. M. H., Bell, M. L. and Finger, T. E. (2003). Disruption of sonic hedgehog signaling alters growth and patterning of lingual taste papillae. *Dev. Biol.* **255**, 263-277.

Hu, B., Nadiri, A., Bopp-Küchler, S., Perrin-Schmitt, F. and Lesot, H. (2005). Dental epithelial histomorphogenesis in vitro. *J. Dent. Res.* **84**, 521-525.

Itasaki, N., Jones, C. M., Mercurio, S., Rowe, A., Domingos, P. M., Smith, J. C. and Krumlauf, R. (2003). Wise, a context-dependent activator and inhibitor of Wnt signalling. *Development* **130**, 4295-4305.

Iwatsuki, K., Liu, H.-X., Grónder, A., Singer, M. A., Lane, T. F., Grosschedl, R., Mistretta, C. M. and Margolskee, R. F. (2007). Wnt signaling interacts with Shh to regulate taste papilla development. *Proc. Natl. Acad. Sci. USA* **104**, 2253-2258.

Kapsimali, M. and Barlow, L. A. (2013). Developing a sense of taste. *Semin. Cell Dev. Biol.* **24**, 200-209.

Kassai, Y., Munne, P., Hotta, Y., Penttilä, E., Kavanagh, K., Ohbayashi, N., Takada, S., Thesleff, I., Jernvall, J. and Itoh, N. (2005). Regulation of mammalian tooth cusp patterning by ectodin. *Science* **309**, 2067-2070.

Kaufman, M. H. (1992). *The Atlas of Mouse Development.* San Diego: Academic Press.

Kawano, Y. (2003). Secreted antagonists of the Wnt signalling pathway. *J. Cell Sci.* **116**, 2627-2634.

Kettunen, P., Laurikkala, J., Itäranta, P., Vainio, S., Itoh, N. and Thesleff, I. (2000). Associations of FGF-3 and FGF-10 with signaling networks regulating tooth morphogenesis. *Dev. Dyn.* **219**, 322-332.

Lintern, K. B., Guidato, S., Rowe, A., Saldanha, J. W. and Itasaki, N. (2009). Characterization of wise protein and its molecular mechanism to interact with both Wnt and BMP signals. *J. Biol. Chem.* **284**, 23159-23168.

Liu, H.-X., Maccallum, D. K., Edwards, C., Gaffield, W. and Mistretta, C. M. (2004). Sonic hedgehog exerts distinct, stage-specific effects on tongue and taste papilla development. *Dev. Biol.* **276**, 280-300.

Liu, F., Thirumangalathu, S., Gallant, N. M., Yang, S. H., Stoick-Cooper, C. L., Reddy, S. T., Andl, T., Taketo, M. M., Dlugosz, A. A., Moon, R. T. et al. (2007). Wnt-beta-catenin signaling initiates taste papilla development. *Nat. Genet.* **39**, 106-112.

Liu, H.-X., Henson, B. S., Zhou, Y., D'Silva, N. J. and Mistretta, C. M. (2008). Fungiform papilla pattern: EGF regulates inter-papilla lingual epithelium and decreases papilla number by means of PI3K/Akt, MEK/ERK, and p38 MAPK signaling. *Dev. Dyn.* **237**, 2378-2393.

Liu, H.-X., Grosse, A. S., Iwatsuki, K., Mishina, Y., Gumucio, D. L. and Mistretta, C. M. (2012). Separate and distinctive roles for Wnt5a in tongue, lingual tissue and taste papilla development. *Dev. Biol.* **361**, 39-56.

Liu, H. X., Ermilov, A., Grachtchouk, M., Li, L., Gumucio, D. L., Dlugosz, A. A. and Mistretta, C. M. (2013). Multiple Shh signaling centers participate in fungiform papilla and taste bud formation and maintenance. *Dev. Biol.* **382**, 82-97.

Maretto, S., Cordenonsi, M., Dupont, S., Braghetta, P., Broccoli, V., Hassan, A. B., Volpin, D., Bressan, G. M. and Piccolo, S. (2003). Mapping Wnt/ -catenin signaling during mouse development and in colorectal tumors. *Proc. Natl. Acad. Sci. USA* **100**, 3299-3304.

Miller, I. J. and Reedy, F. E. (1990). Variations in human taste bud density and taste intensity perception. *Physiol. Behav.* **47**, 1213-1219.

Min, H., Danilenko, D. M., Scully, S. A., Bolon, B., Ring, B. D., Tarpley, J. E., DeRose, M. and Simonet, W. S. (1998). Fgf-10 is required for both limb and lung development and exhibits striking functional similarity to Drosophila branchless. *Genes Dev.* **12**, 3156-3161.

Mistretta, C. M. and Liu, H.-X. (2006). Development of fungiform papillae: patterned lingual gustatory organs. *Arch. Histol. Cytol.* **69**, 199-208.

Miura, H., Kusakabe, Y., Sugiyama, C., Kawamatsu, M., Ninomiya, Y., Motoyama, J. and Hino, A. (2001). Shh and Ptc are associated with taste bud maintenance in the adult mouse. *Mech. Dev.* **106**, 143-145.

Mohammadi, M., Olsen, S. K. and Ibrahimi, O. A. (2005). Structural basis for fibroblast growth factor receptor activation. *Cytokine Growth Factor. Rev.* **16**, 107-137.

Monteiro, A., French, V., Smit, G., Brakefield, P. M. and Metz, J. A. J. (2001). Butterfly eyespot patterns: evidence for specification by a morphogen diffusion gradient. *Acta Biotheor.* **49**, 77-88.

Ohazama, A., Johnson, E. B., Ota, M. S., Choi, H. Y., Choi, H. J., Porntaveetus, T., Oommen, S., Itoh, N., Eto, K., Gritli-Linde, A. et al. (2008). Lrp4 modulates extracellular integration of cell signaling pathways in development. *PLoS One* **3**, e4092.

Peterka, M., Lesot, H. and Peterková, R. (2002). Body weight in mouse embryos specifies staging of tooth development. *Connect. Tissue Res.* **43**, 186-190.

Petersen, C. I., Jheon, A. H., Mostowfi, P., Charles, C., Ching, S., Thirumangalathu, S., Barlow, L. A. and Klein, O. D. (2011). FGF signaling regulates the number of posterior taste papillae by controlling progenitor field size. *PLoS Genet.* **7**, e1002098.

Rothova, M., Thompson, H., Lickert, H. and Tucker, A. S. (2012). Lineage tracing of the endoderm during oral development. *Dev. Dyn.* **241**, 1183-1191.

Shim, K., Minowada, G., Coling, D. E. and Martin, G. R. (2005). Sprouty2, a mouse deafness gene, regulates cell fate decisions in the auditory sensory epithelium by antagonizing FGF signaling. *Dev. Cell* **8**, 553-564.

Thirumangalathu, S., Harlow, D. E., Driskell, A. L., Krimm, R. F. and Barlow, L. A. (2009). Fate mapping of mammalian embryonic taste bud progenitors. *Development* **136**, 1519-1528.

Wilkinson, D. G. and Nieto, M. A. (1993). Detection of messenger RNA by in situ hybridization to tissue sections and whole mounts. *Methods Enzymol.* **225**, 361-373.

Yan, D. and Lin, X. (2009). Shaping morphogen gradients by proteoglycans. *Cold Spring Harb. Perspect. Biol.* **1**, a002493.

Zhou, Y., Liu, H.-X. and Mistretta, C. M. (2006). Bone morphogenetic proteins and noggin: inhibiting and inducing fungiform taste papilla development. *Dev. Biol.* **297**, 198-213.

DEVELOPMENT